-UEQ-90-008
MAY 1990

FOREIGN
BROADCAST
INFORMATION
SERVICE

JPRS Report

Science & Technology

USSR: Engineering & Equipment

Science & Technology

USSR: Engineering & Equipment

JPRS-UEQ-90-008 15 May 1990

CONTENTS

Industrial Technology, Planning, Productivity

UDC 621.735.7:658.52.011.56.012.3

Robot System for Cold End Reeling of Bearing Ring

907F0231A Moscow
KUZNECHNO-SHTAMPOVOCHNOYE PROIZVODSTVO in Russian No 2, Feb 90 (manuscript received 09 Jun 89) pp 30-32

[Article by F. A. Teplyy, V. A. Akopyan, and P. S. Yalanskiy]

[Text] Specialists from the Azov Special Design Office for Press-Forging Equipment and Automated Lines developed a design for a robot system for cold end reeling of a 42726.02 carriage bearing ring.

The 42726.02 is currently manufactured on model L408 lines. The initial blank is a hot-rolled bar of ShKh15SG steel with a diameter of $85^{+0.5}_{-0.3}$ mm and a length between 3,500 and 6,000 mm. The production process consists of the following operations:

—Marking out the measuring blanks by hand and with a gas burnerles on a hydraulic press with a force of 6,300 kN;—Reeling the outer surfaces on a model KPS-250 reeling mill;—Calibrating the inner diameter and height on a press with a force of 2,500 kN.

The system developed is equipped with devices permitting total automation of the processes of loading, reeling, and issuing the finished component.

The production process entailed in cold reeling of a ring's collar (Figure 1 [photograph not reproduced]) consists of localizing the plastic deformation focus created by the reeling roller. The metal fills the space between the face of the shaping roller,[1] the die, and the reeling roller. The area of contact between the reeling roller and blank during the reeling amounts to about 3 to 4 percent of the total area of the ring collar that is being formed.

During the reeling process the die and blank are forced to turn while the shaping and holding[2] rollers are not driven but are instead turned by friction forces.

Depending on the mechanical properties of the material and the configuration and dimensions of the collar being reeled, the design provides for configuring the reeling roller in relation to the blank axis at an angle α with a ranging from 0 to 10 degrees.

The blank undergoing the reeling is a segment of pipe that has been premachined along the outer and inner diameter with a clearance of plus or minus 0.1 mm, a roughness class of 5, the steel ShKh15 (GOST [All-Union State Standard] 801-78) as its material, and an initial hardness of 195.

The following were analyzed during the process of experimental development of the cold reeling technology: production forces, flow of metal, collar deformation time, distribution of hardness along the cross section of the reeled blank, and degree of deformation. The depth to which the roller was introduced into the blank in one rotation amounted to about 0.45 mm. With an introduction of 4.5 to 5 mm the outer diameter of the blank's collar reached the end of the shaping roller, and axial flow of the metal in both directions began. The gap between the end of the shaping roller and reeling roller is filled, as if creating a wedge, by the debending roll, which reduces the precision and increases the labor input required for further machining of the ring. The outer facet of the blank plays a special role in reducing the dimensions of this flash; to the extent possible, it should have the largest allowable dimensions at an angle to the axis of 30-35 degrees.[3]

It takes 15 seconds to reel the collar, which corresponds to 45 rotations of the spindle.

Metallographic studies were conducted to test the reeled rings. The hardness along the cross section was measured on manufactured templates (Figure 2), and the greatest hardness was measured in the region of the reeled collar.

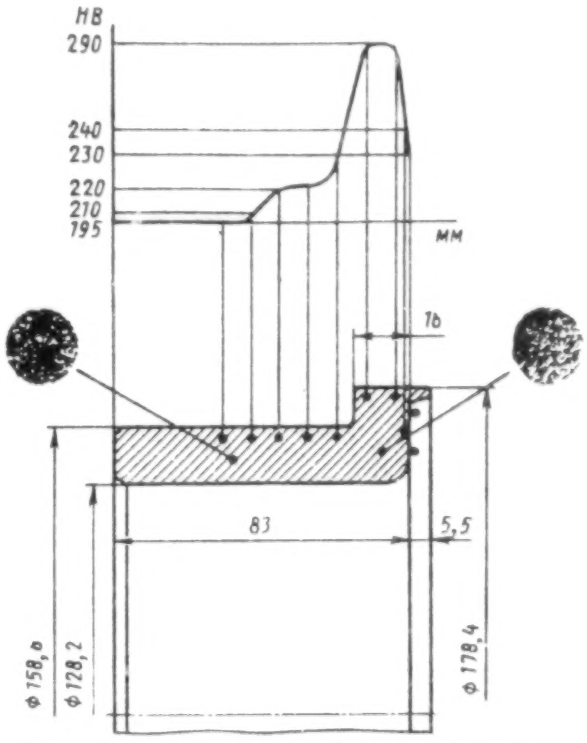

Figure 2. Distribution of Hardness Along the Cross Section of an Uncoiled Blank

The macro- and microstructures at the sites of the greatest and least hardness were studied. No exfoliation or other defects on the reeled components were detected.

An even distribution of stresses at the site of the transition to the collar is needed from the standpoint of strength of the component and the technological force of

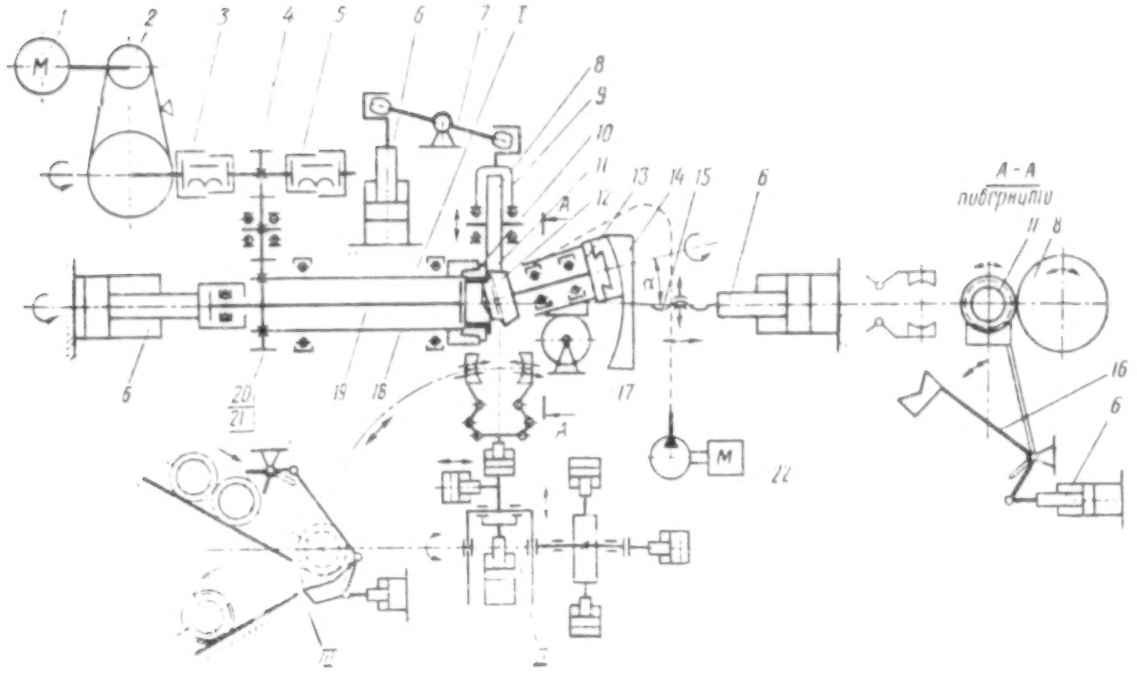

Figure 3. Mechanical Diagram

Key: I. reeling machine; II. industrial robot, III. magazine; 1. 22, electric motors; 2. pulley; 3. clutch; 4. 20, 21, reducing gear pinions; 5. brake; 6. hydraulic cylinder; 7. lever; 8. shaping roller; 9. fork; 10. die; 11. blank; 12. reeling roller; 13. head; 14. ram; 15. adjusting screw; 16. knife edge; 17. holding roller; 18. spindle; 19. pusher

reeling. As is evident from the axial-cross section microsection presented, the metal flow proceeds with the fibers maintaining an uninterrupted course and having a favorable arrangement.

A design for a robot system (Figure 3) that provides complete automation of the reeling production cycle has been developed on the basis of the production process that was worked out.

The system operates as follows (see Figure 3). The blank, which is oriented in the magazine's (III) chute, is transferred (by the industrial robot's [II][4] gripping mechanism) to the reeling machine's (I) controlled knife edge. After the blank has been configured and the industrial robot's movable arm has been withdrawn from the live zone, the blank is automatically thrust into the die. After this, an instruction is issued to feed the head with the reeling roll to the die and to withdraw the knife edge from the live zone. If the head has not come to within 30-35 mm of the blank, the spindle with the die is set into rotation. The spindle is set into motion by an electric motor through a V-belt transmission, clutch, and reducing gear. When the reeling roll comes within 3-5 mm of the blank, the shaping roller feed is switched on, and a time delay controlling the reeling time and lubrication of the tool (die, reeling roll, shaping roll) is simultaneously switched on. T22 lubricating oil (GOST 32-74) is used as a lubricant material for (cooling) the tool.

When the reeling roller comes into contact with the blank, the reeling process proceeds. After the conclusion of the reeling an instruction is issued to withdraw the shaping roller, switch off the casting, and withdraw the head with the reeling roll. When it is withdrawn 25 to 35 mm, an instruction is issued to stop the spindle and simultaneously switch on the brake. If the reeling roll has come to within 5 to 10 mm of the back edge position, an instruction is given to feed a knife edge, after which the reeled component is pushed out onto the knife edge. After the pusher returns, the industrial robot removes the component to the magazine's diversion chute, after which the cycle is repeated.

A special model MA10Ts4201 robot designed by the Planning, Design, and Technological Institute of Forging Robots (in Taganrog) is used in the system for transport robots (loading and unloading). The industrial robot operates in a polar coordinate system, and its actuator has a pneumatic drive (0.4 to 0.6 MPa). The arm, along with its gripping mechanisms and shift module, has two basic motions: longitudinal and vertical. The robot is equipped with a model UTsM-663 program control system that controls the operation of the industrial robot, reeling machine, and magazine.

All of the system's mechanisms, with the exception of the spindle, have hydraulic and pneumatic drives. The circuit has two operating modes, automaton and setup. The electrical circuit provides for light signaling and blocking related to connection of the hydroelectric generating station, the absence of lubricating oil, the status of the industrial robot's drive and the magazine, and the presence of a blank that has not been pushed out of the die.

Concise Technical Characteristics of Reeling Machine

Production force (max.), kN:	
of reeling roller	1,000
of pressing out (pushing out)	500
Blank Diameter, mm:	
outer	158.8
inner	128.2
Wall thickness, mm	15.0
Length, mm	93.2
Workpiece Dimensions of Collar, mm:	
diameter	172.6
width	16.0
height	25.1
Length, mm	83.0
Capacity, h^{-1}	30
Drive capacity (total), kW	75.0
Mass, kg	26,000
Concise Characteristics of Industrial Robot	
Payload,kg	10
No. degrees of freedom	6
Positioning error, mm	+/-0.1
Arm movement:	
horizontal, mm	800
velocity, m/s	1.3
vertical, mm	150
velocity, m/s	0.3
Turn of arm, degree	180
Mass, kg	550
Concise Characteristics of Magazine	
Type	Elbow
Control	hydraulic
Capacity, pieces	11
Mass, kg	500
Overall dimensions, mm:	
left to right	6,100
front to back	2,100

Main Technical and Economic Indicators

Parameter	Model L408 (Basic Version)	Model S04030.Ts1.01 (New Product)
Wholesale price, rubles	354,947	115,600
Total capacity of electric motor, kW	905	108
No. service personnel	8	2
Cost of equipment (including transportation costs) per balance sheet, rubles	408,189	165,626
Average consumption of material per component, kg	11.37	5.25

Conclusions

1. Cold reeling of a 42726.02 bearing ring makes it possible to increase the metal utilization factor by 28-30 percent, reduce the use of metal-cutting equipment by 10-15 percent, reduce overall labor input by 12-15 percent, and increase labor productivity by 1-12 percent.

2. Bearings with reeled rings last 1.3- to 1.6-fold longer.

3. Using industrial robots makes it possible to accomplish the following: increase productivity, improve labor conditions, reduce injuries, reduce the workforce, and increase the capital investment coefficient.

4. The economic effect of introducing a reeling machine into industry when manufacturing a 42726.02 bearing ring amounts to 190,000 rubles per year.

Bibliography

1. USSR Inventor's Certificate 1291260. MKI V 21N 1/06. "Ustroystvo dlya tortsovoy raskatki osesimmetrichnykh izdeliy" [Device for Reeling Axiosymmetrical Products].

2. USSR Inventor's Certificate 1247140. MKI V 21N 1/06. "Ustroystvo dlya tortsovoy raskatki osesimmetrichnykh izdeliy" [Device for Reeling Axiosymmetrical Products].

3. Teplyy, F. A., Yalanskiy, P. S., and Akopyan, V. L., "Machine Tool for Cold Reeling of 42312 Bearing Ring," KUZNECHNO-SHTAMPOVOCHNOYE PROIZVODSTVO, No 5, 1986, pp 37-40.

4. Krivitskiy, A. A., Malkov, Yu. V., Sachkov, A. B., et al., "Promyshlennyye roboty dlya listovoy i obyemnoy shtampovki" [Industrial Robots for Sheet Forming and Die Forging], Moscow, NIImash, 1983, 47 pages.

UDC 621.865.8-229.29.004.14:621.865.8113:621.757.06

Robot Gripping Mechanism

907F0257A Moscow MASHINOSTROITEL in Russian No 2, Feb 90 pp 15-16

[Article by O. P. Stepanov, V. A. Roberov, and V. Ye. Pavlov]

[Text] One promising direction in the development of robotics is that of equipping industrial robots with sensitized pneumatic gripping mechanisms that can be used for sensory control of the end-effector's motion and correct the programmed motions of the end positions of an industrial robot's arms to increase its positioning accuracy and speed. Adaptive assembly gripping mechanisms equipped with pneumatic sensors to scan the mated edges of workpieces in two mutually perpendicular coordinates may be used successfully for robots intended for implementing particularly precise assembly operations.

Working jointly, specialists from the scientific production collective Istok and the Mechanics Problems Institute of the USSR Academy of Sciences developed and manufactured an original design of an adaptive assembly gripping mechanism equipped with a self-contained pneumatic drive and capable of scanning the gripping mechanism along with the workpiece clamped in it within the bounds of several millimeters relative to the workpiece being mated. This kind of adaptation results in a situation wherein the gripping mechanism mounted on an industrial robot's arm with a position or loop control system can achieve a position during which the precision of the industrial robot itself ceases to have a decisive effect on the result of the assembly process since the gripping mechanism's drive fulfills the function of final guidance of the workpiece. In this case the industrial robot's manipulator will only be responsible for making the transport motion entailed in transferring the gripping mechanism, and the function of exact orientation will be assumed by the gripping mechanism's electric drive. Orientation does not require control of all of the links of the industrial robot's manipulator, which results in a reduction of the control device's overall dimensions.

Figure 1 shows the assembly gripping mechanism. It is gripping a workpiece (4) with the four fingers (3) of its lever-and-hinge mechanism, which has a pneumatic drive (2). Mounted to the end of each finger is a sensor (5) that has a nozzle (6) on its end. The industrial robot's manipulator transfers the workpiece to the plane of the workpiece being mated (7), which fulfills the function of a gate for the extent of the working gap S. Each of two opposing nozzles can be exerted relative to the edge of the opening of the workpiece being mated in the position or opposite the gate or else opposite the opening. The sensors are connected with a pressure relay, and because of the resultant mismatch, the gripping device's drive (1) makes it possible to bring the secured workpiece to the axis of the opening of the workpiece being mated.

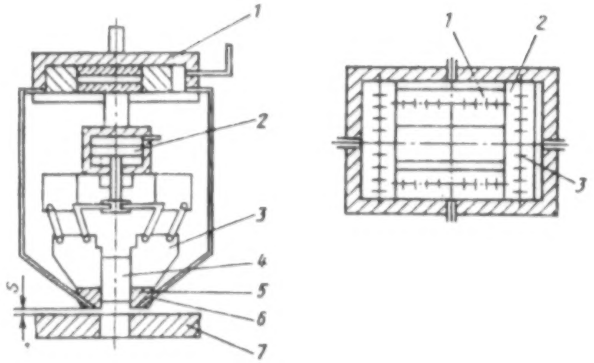

Figures 1 and 2

The design of the gripping mechanism's drive is presented in Figure 2. The drive contains two rams (1 and 2) moving in mutually perpendicular coordinates along the glide planes inside the drive's closed case. Throttle orifices (3) are provided to permit the smooth motion of the rams on all of the contacting planes.

The device that has been developed provides a precision up to 5 microns and a high speed, and it may be used in outfitting any industrial robot equipped with a position or loop control system (TUR-10, TUR-10K, TUR-2.5, Universal-5, etc.) to perform assembly operations.

It is planned that an array of type sizes of adaptive gripping mechanisms with an analogous design for industrial robots with different payloads that are intended for performing a broad class of assembly operations will be developed in the future.

UDC 621.9.06.52

Automatic Rotary Conveyer Line With Flexible Workpiece Stream

907F0234A Moscow MEKHANIZATSIYA I AVTOMATIZATSIYA PROIZVODSTVA in Russian No 10, Oct 89 pp 1-3

[Article by A. N. Mikhaylov, candidate of technical sciences, and N. E. Ternyuk, doctor of technical sciences, under the "Automating Production Processes" rubric: "Automatic Rotary Conveyer Line With Flexible Workpiece Stream"]

[Text] The field of integrated automation of production systems is undergoing qualitative shifts in the direction of the development of such systems on the basis of automatic rotary conveyer lines. The experience that has been accumulated to date with regard to designing, manufacturing, and operating them has posed new tasks in the area of increasing the capacity and expanding the production capabilities of automatic rotary conveyer lines.

In existing automatic rotary conveyer lines the actuators are mounted on the service rotors, whereas the tools configured in the tool blocks are mounted in the sockets of a flexible chain conveyer that passes around the service rotors in specified sections. Only in those sections where the tool-transport conveyer makes contact with the service (production) rotor do the rotor's actuators interact with the respective tools located on the conveyer. Here the transport and production functions are combined in time, and the service rotors turn in step and continuously in relation to one another.

The practice of operating automatic rotary conveyer lines shows, however, that during periods when the tool blocks are replaced while the line is being switched for another product list or when its nodes are being readjusted it is necessary to stop one service rotor (group of rotors) or change the frequency of its (their) rotation relative to the other rotors turning without a change in frequency. In view of the fact that existing lines have their rotors connected with one another by chain conveyers, the rotors rotate in step, and while the line is in operation it is impossible to stop one rotor (group of rotors) or change its (their) rotation frequency relative to the other rotors. This significantly reduces the production capabilities and capacity of automatic rotary conveyer lines. In this respect it has therefore become necessary to implement lines with a flexible stream of workpieces between rotors. Figure 1 is a block diagram of such a line.

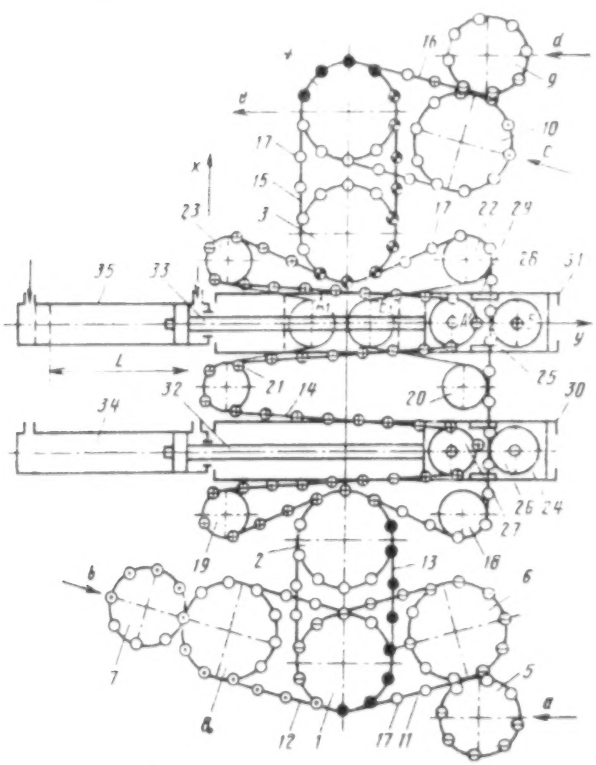

Figure 1. Block Diagram of an Automatic Rotary Conveyer Line

The line consists of production (1-4) and auxiliary (5-10) rotors that are connected with one another by several infinite chain conveyers (11-16) located at different levels. Mounted on the hinged links of each of the conveyers are gripping mechanisms (17) for arranging the workpieces.

A chain conveyer (14), which is located between the production rotors (2 and 3) and which is designed in the form of a storage bin, has nonmovable guide sprockets (18-23) and movable guide sprockets that are mounted on slide rails in pairs (26-27 and 28-29) and that connect the drive and driven arms of the conveyer chain (14). The slide rails are arranged on cross guides (30 and 31) and are connected by rods (32 and 33) to pneumatic cylinders (34 and 35).

The automatic rotary conveyer line operates as follows. Auxiliary rotors (5-8) and chain conveyers (11 and 12) that have gripping mechanisms transfer the workpieces in the incoming streams a and b to the production rotor (1). After being assembled on this rotor, they are fed by the chain conveyer (13) to another rotor (2), from which they are transferred via chain conveyer (14) to yet another rotor (3) for machining. Then a chain conveyer (15) transfers the workpiece to the production rotor (4). Additional workpieces also arrive at this rotor in the incoming streams d and c through the auxiliary rotors (9 and 10). The finished products are unloaded from the line along the outgoing stream e.

When the rotor (2) and its rotor groups (1, 5, 6, 7, and 8) are shut down or when their frequency relative to the production rotor (3) and its groups (4, 9, 10) is reduced, the guide sprockets (28 and 29) move. When this happens, the number of links in the chain is reduced, as is the number of workpieces on driving arm of the chain, and the number of links and workpieces on the driven arm of the chain conveyer (14) is increased, i.e., the storage unit ensures the continuous entry of workpieces into the latter rotor (3) during a shutdown or change in rotation frequency of the former rotor (2). The slide rails (25) are moved along the guides by having the rotor (3) select links of the drive arm of the chain conveyer (14), with the sprocket (28), which moves together with the sprocket (29), keeping the tension of its driven arm constant. The pneumatic cylinder (35) is intended to keep the slide rails' motion resistance constant as it moves to the left or right. When the rod (33) moves its limit amount L, the slide rails (25) and sprockets (26 and 27) move from the position AB to the position A_1B_1. The slide rails (24) and sprockets (26 and 27) move at the same time. The rod (32) and pneumatic cylinder (34) also give the slide rails (24) a constant motion resistance when they move to the left or right. The workpieces proceed to the production rotor, thus ensuring the continuous operation of the line during a shutdown or change in rotation frequency of one of the rotors or a group of rotors along the line.

In the event of the shutdown or reduction in rotation frequency of the rotor (3), all of the operations described above are repeated in reverse order.

As an example we will determine the maximum possible shutdown time for rotor (2) while rotor (3) is operating that is required to replace a malfunctioning tool block on the chain conveyer (13) for an automatic rotary conveyer line assembling an aerosol valve.

The geometric parameters of the automatic rotary conveyer line's components are as follows: pitch of the rotors and conveyer chains, t = 94.2 mm; number of positions on the production rotors (1-4), z = 32; diameter of the production rotors' pitch circle, d_1 = 960 mm; number of positions on the auxiliary rotors (6, 8, and 10), z_2 = 24 mm [sic]; diameter of the pitch circles of the auxiliary rotors (6, 8, and 10), d_2 = 720 mm; number of positions on the auxiliary rotors (5, 7, and 9), d_3 = 430 mm; number of storage units on the chain conveyer (14), p = 10; radius of the pitch circles of the sprockets (18-23 and (26-29), R = 200 mm; half the distance between the centers of the sprockets (21, 23) of one storage unit, x = 600 mm; coordinate of the maximum position of the sprocket (29), y_1 = 3,000 mm; and coordinate of the minimum position of the sprocket (29), y_2 = -R = -100 mm. The nominal rotation frequency of the production rotors is n = 10 rpm. The line's capacity amounts to 19,200 pieces per hour. The linear velocity at which the workpieces move together with the chain conveyer amounts to v = 502.65 mm/s. The formula for calculating the maximum possible time for which rotor (2) can be shut down is

$$T_0 = \Delta l p / v, \quad (1)$$

where T_0 is the rotor's downtime, Δl is the difference in the length of the drive arms of the chain conveyer of one storage unit when the movable sprocket is located in the positions y_1 and y_2; p is the number of storage units on the chain conveyer; and v is the linear velocity at which the workpieces move.

Here the difference in lengths Δl of the drive arms of the chain conveyer of one storage unit is determined by the expression

$$\Delta l = l_1 - l_2, \quad (2)$$

where l_1 is the length of the drive arm of the chain conveyer in the storage unit sprocket position y_1 and l_2 is the length of the drive arm of the chain conveyer in the storage unit sprocket position y_2.

The length of the drive arm of the chain conveyer in each position of sprocket (29) is found by using the following dependence:

$$l_i = 2A - 8R\left[\pi - \left(\operatorname{arctg}\frac{x}{y_i - R} + \operatorname{arctg}\frac{A}{2R}\right)\right], \quad (3)$$

where l_i is the length of the drive arm of the chain conveyer in the i-th position of the storage unit sprocket, R is the radius of the sprockets' pitch circles, x is half the distance between the centers of the storage unit sprockets (21 and 23), and y_i is the coordinate of sprocket (29) in the i-th position.

By substituting expression (3) into (2) and allowing for the fact that in the limit position of the sprocket when y_2 = R the length of the drive arm of the chain conveyer l_2 = 2x, formula (1) assumes the form

$$T_0 = \frac{2p}{v}\left\{A - x + 4R\left[\pi - \left(\operatorname{arctg}\frac{x}{y_1 - R} + \operatorname{arctg}\frac{A}{2R}\right)\right]\right\}, \quad (4)$$

(where)

$$A = \sqrt{x^2 + (y_1 - R)^2 - 4R^2}.$$

The number of workpieces in reserve in the line's storage units is determined from the expression

$$K = \Delta l p / t,$$

where K is the stockpile of workpieces and t is the pitch of the rotors and conveyer chains.

By substituting the numerical values of the line's geometric parameters into formulas (4) and (5), we obtain T_0 = 136.7 s and K = 729 workpieces.

The automatic rotary conveyer line design developed thus makes it possible to stop a rotor (group of rotors) or change the frequency of its (their) rotation relative to the other rotors when readjusting the line's components or when replacing tool blocks while switching the line over for a new product list. In addition, in the event that different rotors (sections of rotors) have different capacities, it is possible to ensure their efficient operation, which is to say, to have one rotor (section of rotors) on a line continue to operate without interruption while another of the line's rotors is stopped for specified time intervals. All of this significantly improves technical and economic indicators, expands production capabilities, and increases lines' capacities.

UDC 621.375.826

Automating and Mechanizing Laser Treatment Manufacturing Processes

907F0234B MEKHANIZATSIYA I AVTOMATIZATSIYA PROIZVODSTVA in Russian No 10, Oct 89 pp 3-6

[Article by A. N. Feofanov and A. A. Uvarov, candidates of technical sciences]

[Text] The welding methods used at the present time are subdivided into two groups: fusion welding (which includes manual covered electrode, manual gas-shielded and submerged, powder wire, electroslag, electron beam, and laser welding) and pressure welding (which encompasses all types of resistance welding as well as welding based on new methods [cold, friction, ultrasound, etc.]), both with and without heating.

The most popular method in machine building is fusion welding (accounting for 67 percent of the total volume of

welding operations), and of all of the types of fusion welding, manual covered electrode welding is most popular (accounting for 65 percent of all metal welded on by all types of welding). Mechanized methods are used to weld on 32 percent of all metal, with the methods of submerged and gas-shielded welding being used on 12 percent. Thirty percent of all welding operations are implemented by using resistance welding, with only 3 percent involving the new methods. Methods of welding by ultrasound, explosion, plasma and microplasma treatment of metals, etc., have been developed. Of these, the plasma and plasma arc welding methods are very interesting. They have much in common with arc welding but have the following characteristic distinction as well: plasma serves as their main source of thermal energy. A plasma stream or jet may be used to treat (weld, cut, spray, solder, heat-treat, etc.) metal and nonmetal (glass, ceramics, etc.) materials.

The following auxiliary operations have a large relative share (about 35 percent of the total labor directly input into welding operations): configuring and positioning workpieces for welding, cleaning edges and seams, configuring an automatic device in the presence of a seam, withdrawing an automatic device, or moving a product. It is precisely for this reason that special attention is being paid to mechanizing welding production, including primary and auxiliary operations.

Calculations have established that when only welding operations are mechanized, the level of integrated mechanization increases by 25 percent, and when auxiliary, transport, and assembly operations are also mechanized, it increases even more. Mechanization of preparatory operations entailing the use of modern equipment to clean and straighten rolled stock, blanks, and workpieces and for unwinding, cutting and bending, stamping and piercing holes, shaving edges, and drilling holes is important for improving the efficiency of welding production.

Above all, integrated automation of welding production itself based on the introduction of automatic welding machines and lines that automatically perform the primary and auxiliary operations entailed in the technological process of welding a product is a necessary condition of any automated welding production.

A loading device ensuring the nonstop, continuous feed of blanks into the machine is a necessary part of welding and welding and assembly machines.

The loading device is equipped with a magazine or bin-type storage unit that serves to store a stockpile of blanks and to remove a single blank at a time and feed it to the machine's live zone. In machines intended for manufacturing products consisting of several identical components, the respective number of blanks is fed into the live zone simultaneously.

Creating building block-type equipment from standardized subassemblies, where making a change for a new type of product dose not require a complete equipment change but only replacement and reconfiguration of its individual subassemblies, is promising. This will make it possible to use automatic equipment under conditions of not only mass but also series production as well.

Unlike electron beam treatment, laser beam treatment does not require vacuum chambers. The process of laser welding is implemented in an atmosphere of air or in a medium of protective neutral gases (Ar, He), a carbon dioxide (CO_2) medium, etc. It thus becomes possible to use laser welding in automated retoolable production to connect structural components with any overall dimensions.

One distinction of laser radiation is that the laser beam can (when mirror optical systems are used) be directed into hard-to-reach places, sent across significant distances without energy losses, and used in several working sections either simultaneously or sequentially. These characteristic features of laser radiation make it possible to automate the laser welding process. The simplicity of controlling the laser radiation's energy characteristics should also be mentioned.

Unlike an electron beam, arc, or plasma, a laser beam has no effect on the magnetic fields of the components being welded or the production equipment, which makes it possible to produce a weld that is stable and of high quality along its entire length.

The principle of laser heat strengthening of metals and alloys based on them entails the action of laser radiation on the surface being treated for a short interval of time. The surface layer of the metal absorbs thermal energy in dimensions sufficient for dissolution of the carbon and implementation of austenitic transformations. During the heating period very large temperature gradients are formed on the surface, which is a necessary condition of rapid cooling by withdrawing heat to the depths of the metal. The hardening process is implemented while the metals are kept in a hot state. Figure 1 presents a comparative diagram of laser treatment of materials. It follows from the diagram that the technological process of heat treatment is implemented at minimal radiation flux densities and a minimal relative duration of the thermal effect (1 to 2 seconds). The maximum depth of the hardened zone lies within the bounds of 1-2 mm. This is fully sufficient to increase durability, strength, and fatigue resistance. The main benefit of a such a treatment method is to keep the main properties of the metal unchanged

Conventional heat treatment methods cause a distortion of the product's shape, and cementation and nitriding are too laborious and time consuming.

The main advantage of the maximum temperature gradients achieved on the object's surface is the fact that there are no energy expenditures to heat the entire layer and, consequently, none for its subsequent cooling in a water or oil bath. The process of heat strengthening is ecologically clean. In addition, the laser beam is the sole option for heat strengthening gray cast iron, which is

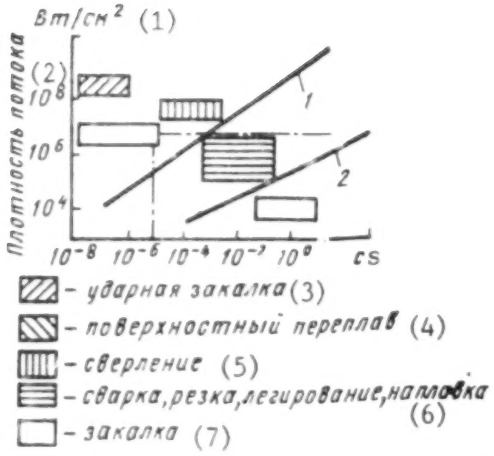

Figure 1. Diagram of the Processes of Laser Treatment of Materials

Key: 1. W/cm² 2. Flux Density 3. Impact hardening 4. Surface remelting 5. Drilling 6. Welding, cutting, alloying, surfacing 7. Hardening

used to manufacture virtually all casing elements of machine tool equipment and the principal mass of slideways.

Two approaches are used when developing the process flow for automated laser treatment of machine tool guides, including built-up guideways. One is based on preliminary application of wear-resistant coatings onto the guides' working surfaces. Plasma spraying of self-fluxing powders on a nickel base is among the most well developed and promising methods of applying coatings that have been subjected to automation and that provide high tribotechnical parameters of the friction pairs. Figure 2 presents an algorithm of the technological process of laser alloying of slideways.

The alloying powder compound may be applied to the guides by automated direct spraying into the laser treatment zone, which naturally increases the consumption of expensive material. It is possible to apply an adhesive compound onto the guides before applying the powder and also to use methods of gas plasma spraying of coatings with subsequent laser beam fusion. The algorithm may vary in terms of the types of finishing treatments of the guides. For example, electroerosion machining, surface plastic deformation, and laser cutting may be used alone or in different combinations. Laser radiation melting of a thin layer of metal and its rapid hardening makes it possible to control the growth of crystals and, accordingly, the metallurgical properties of this layer of metal. Laser alloying the surface of guides helps produce a new exceptionally hard and durable surface with improved fatigue properties. The technological features of this type of approach are, above all, optimal selection of the intensity of the radiation and the time of its effect on the alloyed surface as a function of its effect on the depth to which the metal is melted.

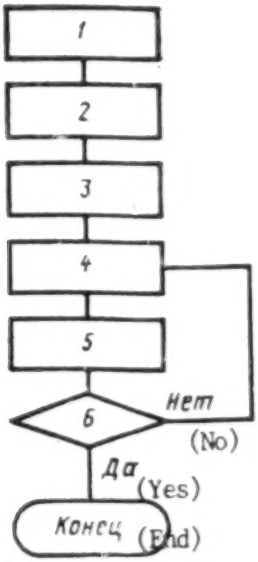

Figure 2. Algorithm for the Production Process of Laser Alloying Slideways

Key: 1. Washing and degreasing 2. Application of alloying compound (powder) onto guides 3. Laser flashing 4. Machining (grinding) 5. Quality control of coating and geometric dimensions of guides 6. Conformity to specifications

Figure 3 presents the dependence of the required radiation intensity (Iα) and duration (4) of the pulse on the thickness (z) of the melted surface layer of the steel. It should be noted that a high surface stress of the metal in the melted state reduces the roughness of the surface being machined.

To reduce the guides' tendency toward seizing, increase their score resistance, reduce the time required for breaking the guides in under the condition of reduced wear during this period, and increase the static contact

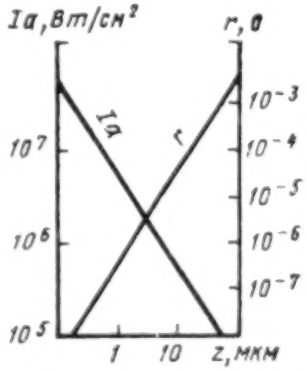

Figure 3. Melting Depth of the Steel (z [measured in μm]) as a function of the intensity (Iα [measured in W/cm²]) and Duration of the Laser Radiation

rigidity of the working surfaces it is possible to recommend another technological approach based on laser hardening of the guides' surfaces with subsequent finishing grinding and finishing laser treatment in a microfusion mode.

Figure 4 presents an algorithm for a simplified version of the technology for hardening built-up machine tool guideways.

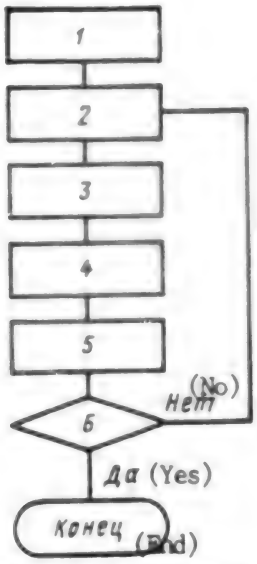

Figure 4. Algorithm for the Technological Process of Laser Heat Strengthening of Slideways

Key: 1. Washing and degreasing 2. Machining of the guides (grinding and scraping) 3. Application of absorbent coating onto guides 3. Laser flashing 4. Laser treatment 5. Monitoring of the geometric parameters and strength characteristics 6. Conformity to specifications

The most significant technological feature of the laser heat strengthening of guides is the well-founded selection of the type of steel and case iron, which should conform to two conditions—hardenability and an ability to absorb laser radiation. The hardenability of steel and cast iron is above all determined by the structure of their crystalline lattice. The diffusion time of carbon is insignificant. Because of this metals with a uniform distribution of carbon are optimum. Rapid austenitization requires a perlite and bainite crystalline structure. Low-carbon steels with a carbon content of less than 0.3 percent are not hardenable for practical purposes. For the machine tool slideways it is advisable to use S416, S421, and S432 gray cast irons; modified cast irons; the carbon and alloyed steels 40, 45, 20Cr, and 18CrMnTi; and the high-carbon alloyed steels ShKh15Sg, KhVG, and 9CrS. Figure 5 shows the dependence of the hardness (HRC) of carbon steels on the percent carbon content (C).

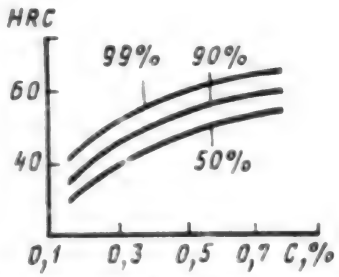

Figure 5. Hardness (HRC) of Carbon Steels as a Function of the Percent Concentration of Carbon (C) During Laser Heat Strengthening

Table 1 presents the hardness values in annealed and laser-hardened material.

Table 1

Material	Hardness (HRC)	
	In annealed state	After laser treatment
S418 cast iron	18-20	65-68
S424 cast iron	24-26	62-63
KaNMU cast iron	22-25	65-68
K435 cast iron	10-14	50-60
35 steel	18-22	53-55
45 steel	18-20	60-65
40Cr steel	81-20	59-60
U8, U9, U10 steel	21-29	up to 72

Lasers with continuous radiation are used to heat treat metals, with single-mode CO_2-lasers being used most often. The wavelength of the radiation of such a laser amounts to 10.6 μm, which corresponds to the range of IR radiation that is visible to humans and requires specific safety measures. The section of the radiation mode is, above all, determined by proceeding from the condition of even distribution of the radiation's intensity and the shape of the hardened zone. The use of single- or low-mode radiation forms a hardened zone with the maximum hardening depth in the center. Consequently, the treated surface will consist of a set of superimposed hardened zones with a nonconstant hardening depth.

The task of increasing the metal's absorptivity entails transferring the maximum amount of laser radiation energy to the material. It should be borne in mind that the amount of energy absorbed depends on the reflective properties of the metal, the oxidation of the surface, the temperature and wavelength of the laser radiation, the electrical conduction of the material, and the surface roughness. Figure 6 presents the qualitative dependence of the absorptivity of the material A on temperature t.

Since the process of heat strengthening is conducted while maintaining the material's solid state, it is limited.

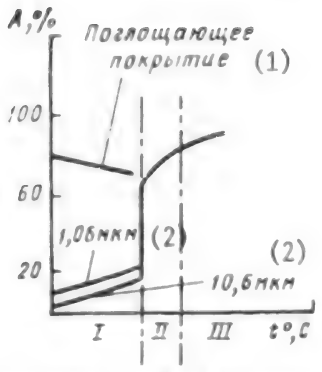

Figure 6. Absorptivity (A) of the Material as a Function of the Temperature and Wavelength of Laser Radiation (I, heat strengthening; II, welding; III, cutting)

Key: 1. Absorbent coating 2. μm

above all, with respect to the density of the energy flux fed to the surface (see Figure 1). For this reason, before laser treatment, a special absorbent coating is applied to the surface (see Figure 6). Graphite, powdered carbon, copper and iron oxides, and other black materials that are easily mixed with quick-evaporating solvents are most often used for these purposes. In specific cases it is possible to use magnesium phosphate, which, besides performing the function of absorbing energy, also visualizes the zone of the heat source's effect. However, applying this substance is an expensive operation. Its use is advisable on critical slideways or when manufacturing guides for special machine tools.

Specified design and technological measures regarding equipping the automated laser unit (Figure 7) should be taken when implementing the operation of the laser heat strengthening of slideways. This laser unit (Figure 7) consists of a production laser (1), an optical system (2) to transmit and focus the laser radiation that includes

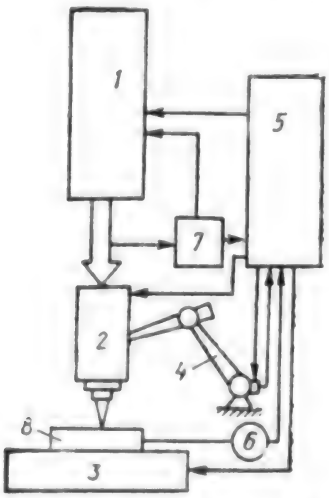

Figure 7. Block Diagram of a Laser Production Unit

lightguides, a mechanized device (3) to secure and move the surface being treated, an automatic manipulator (4) to move the optical system, a programmable controller (5), sensors (6) for the production process parameters (active monitoring), and sensors for the radiation parameters (7).

The laser unit's key technological parameters are as follows: velocity of the laser radiation's movement relative to the workpiece (8) (or vice versa), capacity of the production laser, the laser beam's scanning frequency thanks to the optical system, and extent of the radiation's coverage of the path.

The laser heat-strengthening technology for manufacturing slideways makes it possible to increase the score resistance and static contact rigidity of their working surfaces. Using alloying doping agents also makes it possible to increase the products' corrosion resistance. Built-up guideways can be manufactured from inexpensive soft metals, which saves resources and reduces wastes. Laser heat strengthening is the only possible way of hardening cast iron, with the durability of laser-hardened cast iron guides being increased 8- to 10-fold and that of steel guides being increased 3- to 5-fold when compared with when conventional heat and chemico-thermal treatment methods are used.

UDC 65.04.54:621.643

Mechanizing Expansion of Tubes Into Cone

907F0234C Moscow MEKHANIZATSIYA I AVTOMATIZATSIYA PROIZVODSTVA in Russian No 10, Oct 89 pp 18-19

[Article by G. V. Budkevich, engineer]

[Text] The Minsk affiliate of the all-union scientific research institute Orgstankinprom has designed and manufactured a unit for expanding the steel and copper tubes of hydraulic connections into a cone. The unit was made for the Baranovichi Machine Tool Plant. Compared with forming a cone by the extension method (i.e., the operation of cold stamping, expanding tubes into a cone makes it possible to produce a higher-quality conical tube surface, i.e., one without cracks, breaks, or other mechanical defects.

The unit (Figure 1) consists of an attachment, spindle head, flaring head, drive, and base on which they are mounted.

The attachment is intended to clamp the tubes during the expansion and is a six-position self-centering vise (2) with two pneumatic cylinders, i.e., a tube clamp (14) and regulator to control the course of the clamp (1) to provide the capability of readjusting the attachment for another type size of tube. Each of the vise's positions is intended to clamp a tube with a specified diameter. The vise's positions are marked. The tube clamp's maximum force when the pressure in the unit's is 0.4 MPa amounts to 4,900 N. To readjust the attachment for another type

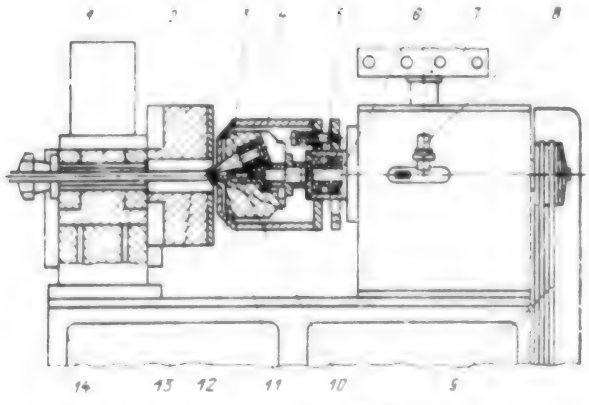

Figure 1. Unit for Expanding Tubes Into a Cone

0size of tube, the vise's half-matrices are parted by a pneumatic cylinder, and the readjustment proper (the turning of the half-matrices) is done by hand, with the angular position of half-matrices being fixed by a spring-loaded latch. After this, a pneumatic cylinder returns the vise's half-matrices to their initial (working) position.

The spindle head transmits the rotary motion from the drive (9) to the flaring head and gives it a forward motion (accelerated feed and working motion) in an axial direction by means of a spindle (5) mounted in a poppet sleeve (6), which is the rod of the pneumatic drive's hydraulic power cylinder. The speed at which the poppet sleeve moves and, consequently, that of the flaring head are regulated by hydraulic equipment. The maximum axial flaring force developed by the poppet sleeve amounts to 3,770 N.

The flaring head consists of three working rollers (3) and a central supporting roller (11) that makes contact with them and that is mounted in a casing (12). A spring-loaded vessel (4) with an inner conical surface touching the surface of the working rollers and setting them into rotation is mounted from the outer side of the casing. To increase the flaring head's reliability, the central supporting roller is equipped with an additional support (10) that is mounted on the central roller at the base of the working rollers.

Table 1. Technical Characteristics

Rotation frequency of flaring head, min^{-1}:	
For pipes 6x0.8; 8x1.0; 10x1.0; 12x1.0	700
For pipes 14x1.0; 18x1.5	500
Capacity of unit, pieces/h	180
Overall dimensions of unit, mm	850x845x1,500
Mass of unit, kg	460

The unit operates in a semiautomatic mode. The tube being expanded (13) is mounted by hand in an attachment before a stop. A spindle rotation speed switch on the control panel (7) establishes the necessary rotation speed for the flaring head. After this, the semiautomatic operating mode is switched on. The tube is clamped in the attachment's vise. When a pressure of 0.4 MPa is reached in the pneumatic network, the drives rotating and moving the flaring heads are switched on. The head's speed is faster at the moment when it first begins moving than during the flaring process. The tube is expanded until the poppet sleeve reaches the end switch (8). The machining of the tube's cone continues for some time with the poppet sleeve not moving. Then, the poppet sleeve and, consequently, the flaring head return to the starting position. In the poppet sleeve's starting position the drive's motor is disconnected, and the attachment's vise is released, thus freeing the machined tube. In the event of an emergency shutdown of the operation, the flaring head—regardless of the position in which it is located—withdraws to the starting position, the drive is switched off, and the vise is opened.

A high quality of tube expansion is achieved thanks to the original design and optimally selected parameters and characteristics of the unit: the rotation frequency of the flaring head, the feed value selected for the flaring head, and the conicity angle at the crest of the working rollers.

The unit makes it possible to flare tubes with confidence, a feat that no other designs can duplicate in view of the unsatisfactory nature of their results.

This unit may find wide-scale use at any of the country's machine building enterprises producing equipment with pneumatic and hydraulic components.

UDC 621.867-81

CAD of Overhead Load-Carrying Conveyers

907F0234D Moscow MEKHANIZATSIYA I AVTOMATIZATSIYA PROIZVODSTVA in Russian No 10, Oct 89 p 22

[Article by V. K. Vasilyev, K. G. Topolidi, and L. Y. Syrkovskaya, candidates of technical sciences]

[Text] One of the laborious sections of designing conveyer transport devices is the traction calculation. The amount of such calculations increases as the route along which the cargo moves increases. Using a computer when making design calculations for overhead load-carrying conveyers, which are widely used at enterprises in different sectors of industry, makes it possible to reduce time expenditures and to make an optimal decision. Unlike the conventional method of making a traction calculation by going around the loop without using a computer, where 10 different equations are generally used, the program for making the calculations on a computer stipulates the use of the following three generalized equations:

—to determine the motion resistances in the sections

$$W_i = q_i (c_i l_i + h_i) + q_{ki} c_i v h_i,$$

—to determine the tension of the pull chain at the end of a section during calculations based on the direction of the conveyer's travel

$$S_i = c_i S_{i-1} + W_i,$$

—to determine the tensions in the beginning of a section during calculations against the travel of the conveyer

$$S_{j-1} = -W_j + S_j/c_j,$$

where i and j are the indexes of the sections' boundaries; q_i is the running linear load from the moving masses, N/m; q_K, is the linear load on the vertical sections of the drops or rises from the pressure of the rollers on the running path, N/m; c_0 is the coefficient of the resistance to motion on the rectilinear sections; l_i is the section length (projection on the horizontal), m; h_i is the difference in the levels of the beginning and end of the section, m; and c_i is the motion resistance coefficient in a curvilinear section.

To use these equations, the conveyer's route is divided into rectilinear and curvilinear sections. This includes a breakdown of the sloped and vertical sections with bends at three sections: the bend at the entry, the rectilinear bend, and the bend at the exit. The specified change dose not affect the essence of the method of traction calculation (without a computer) or its precision.

The following input data identifiers are used in the program compiled on the basis of the algorithm depicted in Figure 1: n, number of points in the conveyer's loop; P_z, specified unit capacity, pieces per hour; x, capacity safety factor; v, conveyer velocity, m/s; t_{min}, minimum suspension spacing, m; t_c, chain pitch, m; m_c, m_k, m_n, m_g, mass of pull chain, carriage, suspension, and cargo, kg/m; g = 9.81 m/s^2, l_{load}, size of load (suspension) along conveyer's length; T_ipC, type of pull chain (for the two-hinge type [D200], T_ipC = 1; for split and plastic chains, T_ipC is unequal to 1); S_p, chain-breaking load, N; y, chain strength safety factor, N; S_{min}, initial chain tension, N; K_{loss}, coefficient of the losses in the drive shaft; Ψ_{drive}, efficiency of the drive; $[P_{li}]$, load factor for the section; $[\beta_i]$, central angles of the vertical bends; $[l_i]$, length (projections on the horizontal) of the sections; $h_i]$, difference between the sections' levels, m; and $[c_i]$, motion resistance coefficient in the curvilinear sections.

The following are determined during the process of implementing the CAD program: the spacing of the carriages t_k and the suspensions t, the design capacity of the conveyer P_k, the running linear loads in the sections g_i, the motion resistance in the sections W_i, the tension of the chain S_i, and the power consumption of the electric drive motor $P_{elec\ mot}$. The program provides for replacing the initial point of the calculation if the running tension of the chain is smaller than the initial tension S_{min}. The pull chain is tested with respect to the allowable load S_{all}. In the case where the chain's tension exceeds the allowable load, the message "chain not strong enough" appears, and the calculation is stopped.

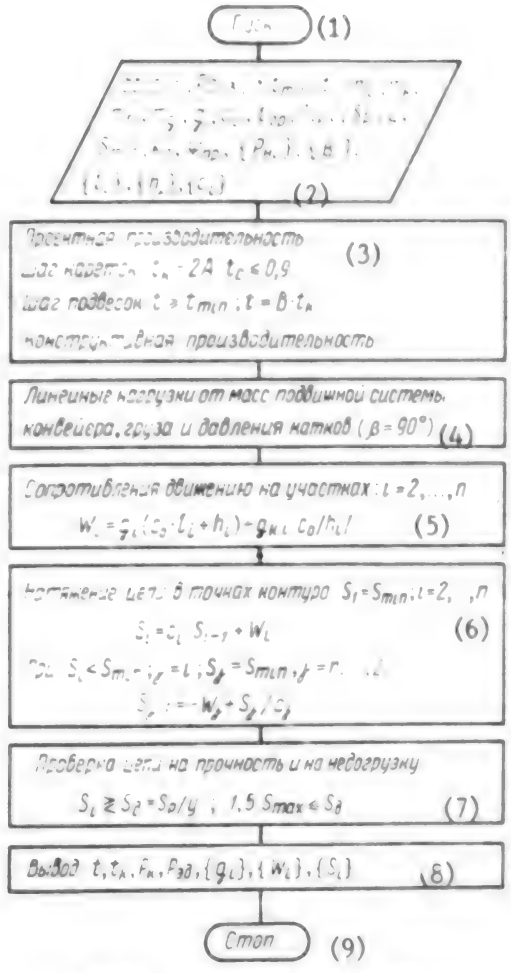

Figure 1. Algorithm for the Program

Key: 1. Start 2. Input: n, Pz, x, v, t_{min}, t_c, m_c, m_k, m_n, m_g, g, c_0, t_{load}, T_ipC, Sp, y, S_{min}, k_{ss}, Ψ_{drive}, $[P_{li}]$, $[\beta_i]$, $[l_i]$, $h_i]$, $[c_i]$ 3. Design capacity; Spacing of carriages: $t_k = 2A$. t_c is less than or equal to 0.9; Spacing of suspensions: t is greater than or equal to t_{min}; $t = \beta$. t_k; Design capacity 4. Linear loads from the mass of the moving system of the conveyer, cargo, and pressure of the rollers (β = 90°) 5. Resistance to motion in the sections: i = 2, ..., n; $W_i = g_i(c_0 . l_i + h_i) + g_{ki} . c_0/h_i/$ 6. Tension of the chain at points of the loop: $S_i = S_{min}$; i = 2, ..., n; $S_i = c_i . S_{i-1} + W_i$ when $s_i < S_{min}$; $j = i$; $S_j = S_{min}$; $j = n, ..., 2$; $S_{j-1} = -W_j + S_j/c_j$ 7. Testing the chain for strength and for underloading: S_i is greater than or less than $S_{all} = S_p/y$; $1.5S_{max}$ is less than or equal to S_8 8. Output: t, t_k, P_k, $P_{elec\ mot}$, $[J_i]$, $[W_i]$, $[S_i]$ 9. Stop

If the maximum load on the chain is 1.5 times the allowable load, a recommendation to select a lighter chain is issued.

The results of the calculation plus the input of specific data are examined by way of the example of an overhead

load-carrying conveyer, and a printout of the values in order of their representation and observance of their dimensionalities is obtained.

Performance of the calculations for the conveyer yield the key characteristics required for further developments. A repeat traction calculation was performed on the basis of the version entered in the program because, in the first calculation, the tension at one of the conveyer's points turned out to be smaller than the initial tension.

The proposed method of designing overhead load-carrying conveyers on a computer may serve as a foundation for creating a series of programs for designing other types of chain conveyer devices.

UDC 658.52.011.56.012.3

A Program Package for Computer-Aided Design of Flexible Manufacturing

907F0233 Moscow MEKHANIZATSIYA I AVTOMATIZATSIYA PROIZVODSTVA in Russian No 2, Feb 90 pp 34-36

[Article by engineers A. V. Bogoyavlenskiy, N. Sh. Ardashirov, and I. M. Khramov]

[Text] The process of creating flexible manufacturing systems (FMS) is rather complicated and includes several stages. From the very first stage—the design—it is necessary to tie together the aspects of choice of parts, processing technology, workload and attendance of the machines, operation of the transport and materials handling system, and others. Furthermore, maximum efficient use should be made of the capital investments. In view of this, it is necessary to develop and analyze several versions of FMS, choosing the best by comparing a series of indexes.

In the traditional method of manual design, the versions of FMS are worked out in succession (one after the other) until the version is found which meets the given specifications. Thus, the labor costs of highly qualified engineers are very large.

The computer substantially reduces the labor expenses and the time involved in creating FMS versions, making it possible to analyze a large number of possible alternatives of flexible manufacturing system and choose the best one in a more scientific way.

The department of metalworking machines and tools of the Ural Polytechnical Institute ha developed a FMS-CAD program package (hereafter, the package), intended to computerize the routine chores of the process engineers in the design of flexible manufacturing systems for machining. It can also be used for design of production sectors and departments with the usual organization of work.

The package automates a sizeable portion of the computations and is used to calculate the parameters of the FMS with optimization of the equipment layout; to compare the sectors that have been developed in terms of criteria; to calculate the economic indexes of the FMS; to simulate in detail the functioning of the flexible manufacturing modules and lines; to simulate flexible automated sectors.

The package may be divided into a number of separate CAD subsystems: one for consolidated calculations of the FMS; one for economic analysis; one for simulation modeling of the FMMs; and one for simulation modeling of the FMS.

A block diagram of the package is shown in the figure.

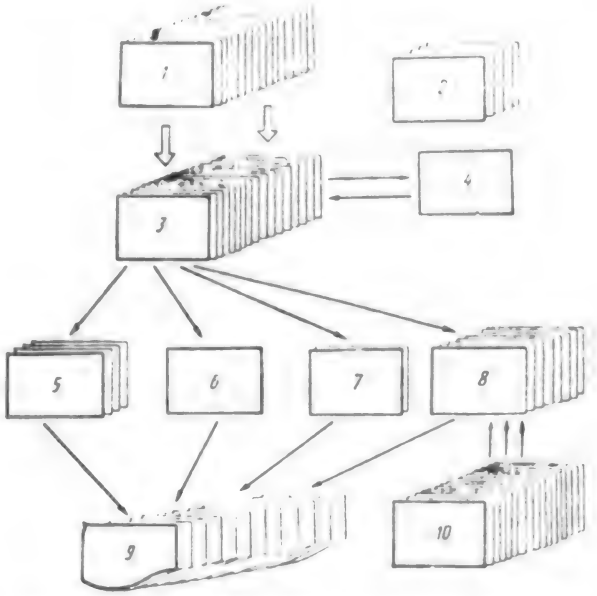

Block Diagram of the FMS-CAD Program Package

Key: 1. Interactive initial-data entry programs 2. Utility programs 3. Initial-data tabular files 4. Data-file screen editor 5. Calculation and optimization of FMS parameters 6. Economic analysis 7. Simulation models of the workload of the sector 8. Simulators of the FMS, FAL, FAS 9. Files of listings with results of computations 10. Simulators of individual devices and operations

Each of the subsystems may be used as part of the package or separately.

The package has a database in the form of tabular text files, created by respective interactive entry programs. The data files after being created can be viewed on the display screen, printed out, and corrected by the screen editor.

Since the design process of the FMS goes through several stages in succession, and the FMS design itself becomes ever more complicated, i.e., new data continually

appear, the package adopts a mode of successive expansion of the initial data, some of which are the outcome of the work of the previous stages.

All the programs of the package work in interactive mode, geared to a user whose profession does not involve a computer.

The subsystem of consolidated calculations is designed to compute the parameters of flexible automated sectors, lines, departments, and machining processes.

The calculations give rise to the following data:

for the machine tools: the overall time to machine parts at each machine group; the number of part-operations assigned to the machine group; the number of types of adjustments for each machine group and for the sector as a whole; the time spent on readjustment of the machines of each group; the total time of utilization of the machines and the number of machines in each group for a given maximum utilization factor; the actual coefficient of utilization of the machines of each group;

for the machine parts: the time of the machining cycle for the part production lot and the processing time for the transport lot;

for the transport: the transport links within the FMS; the travel time up to each group of machines; the overall travel time of the stackers and the transport carts; the number of loading-unloading cycles; the time spent on all operations; the required number of stackers and transport carts and their actual workload factor;

for the materials handling: the overall size of the station; the size of the operational and backup sections; the number of compartments for tools and fixtures; the total number of bins in the sector, in repair, and at the machines. After this, the number of attendants for the FMS is computed.

To compare the different FMS versions, a program is used to calculate generalized criteria of evaluation of the developed FMS version.

Calculation of the parameters of different FMS and comparison of them enable choice of a rational configuration of the FMS and a proper workload of the equipment. The programs are designed for repeated computation of alternatives with different input data.

After the size of the materials handling station, the number of machines and other processing equipment, and the transport system have been chosen, it is possible to move on to optimization of the equipment spacing in order to minimize transport costs. The program provides for two optimization modes: automatic and interactive. As shown by experience, optimization of the equipment spacing makes it possible to shorten the travel time by a factor of 1.5-2.

Furthermore, the subsystem has utility subprograms for automated calculation of the number of parts in a bin, the size of the part production lot, and so on.

In order to assess the economic effectiveness of the developed FMS version, there is the economic analysis subsystem, which computes the economic indexes of the FMS and compares them with the indexes of a reference version.

For a definitive answer to the question as to the operability of the FMS, a computer simulation is carried out. Of major significance here is the accuracy of the initial data and the adequacy of the model to the actual FMS. Since different requirements are placed on the models during simulation of the FMS and different goals are pursued in the investigation, the simulation models should differ in terms of the level of detail and the capacities for control of the input data. In accordance with these requirements, the program package includes different simulation subsystems.

The FMM simulation subsystem makes it possible to simulate the functioning of any given flexible manufacturing module with a high degree of detail. The programs are built on the modular principle, each of them describing a particular device (accumulator, robot, machine spindle, tool drum, etc.) or operation (sampling inspection of parts, tool change, machine adjustment, servicing of the accumulator, etc.).

In a simulation model it is possible to trace the operation of all devices in a dynamic setting, to print out a cyclogram of the operation of the FMM, to model the operation under different tool assemblages and different arrangement of the tools in the drum, to compare different versions of the part machining technology, and to select parts that are most easily machined in this module.

If necessary, the modules can be used to construct a simulation model of a flexible automated sector (FAS). The simulation model of the FAS further includes subroutines which simulate the materials handling station, the stacker, the transport cart, and so on. The subsystem for simulation modeling of flexible automated sectors makes it possible to reduce possible equipment standstill and eliminate bottlenecks by varying the size of the part production lots and their sequence, to evaluate the operation of the FAS in a dynamic setting, and to construct a rational operation schedule for the sector.

The simulator makes it possible to model consecutive and parallel- consecutive processing of the part production lots.

Thus, the program package encompasses all functions—from the feasibility study for creation of the FMS to the resolution of questions involving rational utilization of a sector under development or already existing.

As shown by a preliminary evaluation, the programs of the package reduce the time to design a sector by a factor

of 8-10, compared to manual design; an even greater impact is achieved in the design of a department.

The techniques for design of flexible automated manufacturing and conventional manufacturing are not very different, so that the programs of the package can be used with equal success for the design and simulation of both FMS and conventional manufacturing.

The programs have been developed for computers of type SM-4 and SM-1420, but the limited RAM of these machines prevents development of the utility capabilities of the programs. Work is presently under way to convert the package to IBM-PC type equipment, thus greatly amplifying the program capabilities.

Abstracts From 'Bulletin of Higher Educational Institutions: Machine Building'

907F0241A Moscow IZVESTIYA VYSSHIKH UCHEBNYKH ZAVEDENIY: MASHINOSTROYENIYE in Russian No 11, Nov 89 p 3

[Abstracts appearing in "Bulletin of Higher Educational Institutions: Machine Building," Nov 89]

[Text]

UDC 539.384.1

Strength and Rigidity of Structural Elements Having Shape of Rod With Large Curvature. V. I. Fomin, candidate of technical sciences, pp 3-7

This article analyzes the use of the hypothesis of plane cross section for a plane rod with a large curvature in the general case of loading. Relationships are derived for determining stresses, potential deformations, and movements. They are universal and convenient for practical use. Figures 3, references 3 (Russian).

UDC 620.178.6

Investigation of Stress-Strained State of Surface Layers of Hardened Components. V. G. Kaplun, candidate of technical sciences and docent, V. L. Marchenko, candidate of technical sciences, and Yu. I. Shalapko, engineer, pp 7-10

This article discusses the results of a study (using the finite elements method) of the stress-strained state of the surface layers of components that have been hardened by ion nitriding. It is shown that the thickness of the internal nitriding zone has a significant effect on the distribution of stresses along the component's cross section. Recommendations are given regarding selecting a nitriding process. Figures 3, references 3: 2 Russian, 1 Western.

UDC 539.374+539.4

Strengthening and Accumulation of Damages in Construction Materials During Loading. N. S. Mozharovskiy, doctor of technical sciences and professor, N. I. Bobyr, candidate of technical sciences and docent, and O. N. Mukoida, graduate student, pp 10-15

This article proposes a version of plastic flow theory with a Mroz hardening law that considers the material susceptibility to damage for a refined description of the elastoplastic processes of complex loading.

The article describes a criterion for the limiting state of the material reflecting the loading history. Thin-walled tube-shaped specimens loaded with an axial force and internal pressure along various trajectories were used for experimental verification of the kinetic equation for the accumulation of damage in the material. Figures 2, table 1, references 21: 18 Russian, 3 Western.

UDC 621.787:539.319

Effect of Residual Stresses on Endurance Limit of Component With Rectilinear Cross Section and Concentrator. V. F. Pavlov, doctor of technical sciences and docent, V. I. Lapin, engineer, and S. A. Bordakov, graduate student, pp 16-19

This article proposes a method of calculating the increments of the endurance limit of a hardened component with a rectilinear cross section and with a concentrator that considers the nature of the distribution of residual stresses along the thickness of the component's surface layer. Figures 3, tables 2, references 6 (Russian).

UDC 539.376

Determining Time to Fracture Under Conditions of Creep. V. P. Poshivalov, candidate of technical sciences, pp 19-23

This article examines a probability model of long-term strength. Yu. N. Rabotnov's equations for creep and long-term strength are used. The mean time to fracture of a specimen and its mean square deviation are determined. Theoretical calculations are compared with the results of long-term strength tests on specimens of 12Cr18Ni10Ti steel. Figures 2, table 1, references 6 (Russian).

UDC 539.376

Forecasting Individual Reliability of Structural Elements During Creep in Operation Stage on Basis of Leader. V. P. Radchenko, candidate of technical sciences and docent, and G. A. Pavlova, graduate student, pp 23-27

This article proposes a phenomenological stochastic model of the creep of structural elements that links generalized loads with generalized movements. It is used as the basis for developing a method to estimate the individual reliability of a specific product with respect to its technical status based on data from strain measurement in the initial stage of its operation and information about the creep of a leader-product that had previously

begun operation under identical conditions. An experimental verification of the method is performed. Examples of the calculation are presented. Figures 3, references 9 (Russian).

UDC 539.3

Numerical Analysis of Processes of Axiosymmetrical Shape Change of Thin Shells Based on Viscoplastic Models of Material. L. G. Sukhomlinov, candidate of physical and mathematical sciences, and V. K. Engelsberg, engineer, pp 27-32

A previously developed finite element system for automated calculation of the stress-strained state of thin shells in processes of axiosymmetrical shape change under the effect of rigid dies and hydrostatic pressure is generalized for the case of viscoplastic material. This article examines problems about the shape change of shells made of sheet materials that are sensitive to the deformation rate in a cold state and also in a superplasticity state. The article gives a comparison with existing calculations and experimental results. Figures 3, references 7: 3 Russian, 4 Western.

UDC 539.4

Combined Calculation of Axiosymmetrical Anisotropic Shells With Little-Compressed Filler. V. I. Arbuzov, engineer, A. G. Bakhtin, candidate of technical sciences, and V. I. Gafinov, candidate of technical sciences and docent, pp 32-36

This article examines a calculation method based on a unified scheme. The finite elements, shell, and three-dimensional finite elements methods are used. A comparison of the test results is performed. Figures 3, references 6: 5 Russian, 1 Western.

UDC 539.374

Experimental Determination of Deformations During Combined Extension. K. A. Kaumetov, engineer, pp 36-40

This article examines a method of applying a dividing mesh by using a laser. The article presents the results of determining deformations during combined drawing and draws conclusions regarding the resultant data. The pros and cons of the proposed method are presented Figures 3, references 6 (Russian).

UDC 621.791.052

Brittle Fracture Resistance of Butt Joints With Nonuniform Thickness. A. V. Kolesov, engineer, and K. M. Gumerov, candidate of technical sciences, pp 40-42

This article develops a method for computational assessment of the strength of structural elements with stress concentrators of a two-sided angle with an acute vertex type. An engineering method is proposed for calculating the strength of a butt joint of elements with different thicknesses that is based on the use of the known characteristics K_c (fracture toughness) and σ_B (ultimate strength). Figure 1, references 7: 6 Russian, 1 Western.

UDC 621.833.3

Determining Key Parameters of Transmission with ZT Worm. I. A. Krivenko, doctor of technical sciences and professor, pp 43-47

This article presents a method that makes it possible, as early as in the stage of designing a ZT transmission, to determine that combination of key parameters that ensures that the worm will have the required rigidity. A sample calculation is presented, and the effect of different parameters on a worm's rigidity is analyzed. Figures 2, references 6: 4 Russian, 2 Western.

UDC 519.2:621.81.002.22

Integrated Program for Correlation and Regression Analysis of Results of Mechanical Tests. M. G. Stakyan, candidate of technical sciences and docent, and L. G. Oganesyan, graduate student, pp 47-53

This article examines a method of processing test results in the presence of a linear correlation connection and the constancy of their variances. The problem is solved for a limited and large number of samples (n being less than and greater than 50). The article presents the optimum selection of a linearizing function. An integrated computer algorithm is developed for certain types of tests implemented on a computer. Figures 3, table 1, references 7 (Russian).

UDC 532.62:621.039.5

Effect of Additional Wetting on Chilling of Tube Bundle in Event of Bottom Feed of Liquid. B. G. Ganchev, doctor of technical sciences and professor, A. R. Amirov, engineer, and O. V. Pyatov, engineer, pp 54-58

This article presents an experimental investigation of the chilling of a bundle of tubes in the event of a bottom feed of liquid. The bundle's chilling time is determined by the speed of the main wetting front and by the passage of additional fronts. The presence of spacing grids results in an increase in the mean coefficient of heat release in the supercritical region. Figures 3, table 1.

UDC 621.514

Experimental Investigation of Process Suction of Dry Compression Cold Compressor With Asymmetrical Tooth Profile. V. I. Pekarev, candidate of technical sciences and docent, V. I. Vedayko, candidate of technical sciences, and A. N. Noskov, candidate of technical sciences, pp 58-62

This article examines a method of determining the resistance of different sections of the suction path of a dry compression cold screw compressor. The article presents the resistance coefficient of the compressor's suction chamber and the resistance coefficient when steam moves in the screw spaces as functions of the

Reynolds number. The article provides an analysis of the compressor's volumetric losses in different sections of the suction path. Figures 3, references 5 (Russian).

UDC 62-762

Packing Rolling Elements of Piston Pneumatic Devices. M. A. Kozlovskiy, candidate of technical sciences and docent, pp 63-66

This article examines elastic packing rings with a toothed cross section that have been mounted with their projections having the capability of interacting with annular notches on the sealing surfaces of the piston and housing.

The article presents a calculation of the geometric parameters of the ring and the elastic deformation forces. Figures 2, references 2 (Russian).

UDC 621.671:532.5

Centrifugal Inclined Archimedian Screw Pump With Improved Anticavitation Qualities. A. M. Gorshkov, candidate of technical sciences and docent, M. Yu. Kolpakov, graduate student, and L. V. Khmara, engineer, pp 66-69

This article examines the reasons for the occurrence of cavitation of cryogenic liquids in centrifugal pumps.

The article derives the optimum characteristics of the profile of the blades of radial-axial wheels for pumps with the possibility of manufacturing them on machines with program control. Figures 3, references 2 (Russian).

UDC 621.436.03

Simplified Mathematical Model of Fuel Injection in Diesels With Allowance for Gap Between Body of Suction Valve and Pump Plunger's Bushing. Yu. Ya. Fomin, doctor of technical sciences and professor, Ye. Ya. Karpovskiy, doctor of technical sciences and professor, and V. G. Ivanovskiy, candidate of technical sciences and docent, pp 70-73

This article presents a simplified mathematical model of the process of fuel injection in diesels at the Bryansk Machine Building Plant Production Association with an allowance for fuel leaks through the gap between the body of the suction valve and the bushing of the high-pressure pump's plunger. Figures 3.

UDC 621.436:536.24.023

Investigation of Hydrodynamics and Heat Transfer in Cooling Channels of Diesel Cylinder Heads. A. L. Novennikov, candidate of technical sciences and docent, and A. A. Ivnev, engineer, pp 73-78

This article discusses the results of a study of hydrodynamics and heat transfer in the short drilled cooling channels of diesel cylinder heads. Dependencies are presented for calculating the local heat release coefficients along the channel's length in a forced convection mode. Figures 3, references 3 (Russian).

UDC 62-226:539.384

Antisymmetrical Deformation of Turbomachine Disks. Kh. Sh. Gazizov, candidate of technical sciences and docent, and N. F. Lyashevskiy, engineer, pp 78-81

The problem of antisymmetrical deformations is solved with an allowance for centrifugal forces. It is shown that the real bends and internal moments and forces of rotating disks that are transmitted to the supports are significantly smaller than those obtained on the basis of equations of the classical linear theory of buckling. Figures 3, references 4 (Russian).

UDC 629.113.027:534

Effect of Compliance of Drive of Drive Wheels of Front-Wheel Drive Vehicle on Their Vibrations in Plane. A. S. Otarov, candidate of technical sciences, and G. T. Buniatishvili, graduate student, pp 82-85

This article presents the results of an experimental investigation of the effect of the compliance of the drive of the drive wheels of a front-wheel drive vehicle on their vibrations in a plane.

It is shown that, in view of the nonidentical rigidity of the semiaxles, there occur simultaneous fluctuations of the torques of the semiaxes and wheels in a plane that must be considered when designing front-wheel drive vehicles. Figure 1, references 3 (Russian).

UDC 629.114

Determining Intensity of Wear of Components and Machine Tie-ins. F. N. Avdonkin, doctor of technical sciences, pp 85-88

This article discusses a method for analytical and experimental determination of the magnitude of the intensity (rate) of wear with maximum precision based on scientifically well founded laws of the wear of a component in the process of machines' operation. Figure 1, references 4 (Russian).

UDC 629.114.4.073.001.24

Mathematical Estimate of Controllability of Large-Payload Three-Link Autotrains. Ya. Ye. Farobin, doctor of technical sciences and professor, Yu. L. Zelenin, candidate of technical sciences, and A. S. Budagyan, graduate student, pp 89-94

This article examines software for simulating the motion of a three-link autotrain and presents the results of a study of the controllability of a two- and three-link autotrain. Controllability is assessed on the basis of the latest recommended standards for characteristics and indicators. The possibility of improving the controllability of two- and three-link autotrains by taking the respective technical measures is confirmed. Figures 3, references 4 (Russian).

UDC 629.1.075

Mathematical Model of Curvilinear Motion of Transport Caterpillar Machine Machine Along Deformable Base. V. I. Krasnenkov, doctor of technical sciences and professor, S. A. Kharitonov, candidate of technical sciences, and A. V. Shumilin, engineer, pp 94-99

This article proposes a system of differential equations for the curvilinear motion of a transport caterpillar machine along a deformable base with an allowance for the slippage and sliding of the supporting arms of the caterpillar propeller. A comparative analysis of the processes of the formation of the parameters of the caterpillar machine's turning obtained on the basis of calculations based on a proposed mathematical model and experimentally made it possible to assess the effect of different assumptions on the degree to which the calculated characteristics of the curvilinear motion of a caterpillar machine approximate its real characteristics. Figures 3, references 8: 7 Russian, 1 Western.

UDC 621.8

Selecting Optimal Rigidity of Rubber and Metal Hinges of Sieve Boot of Don-1500 Combine. D. M. Kukichev, candidate of technical sciences and docent, and V. A. Nikonorov, candidate of technical sciences and docent, pp 100-108

This article examines the dynamics of the motion of the multilink lever mechanism of the sieve boot of a DON-1500 combine with an allowance for its elastic rubber-and-metal hinges. The calculations showed that the dynamics loads (in view of the inertial forces) of the most massive links are very significant and may exceed the forces of the technological resistance and static load from the force of gravity. This dynamic load may be reduced by correctly selecting the radial rigidity of the rubber-and-metal hinges. To determine the optimal rigidity of each rubber-and-metal hinge, a four-mass dynamic model of the given mechanism was developed, and a system of differential equations describing the motion of the most massive links with an allowance for the rubber-and-metal hinges was compiled. Specific recommendations are given regarding the optimal radial rigidity of each rubber-and-metal hinge, and this will make it possible to significantly reduce the inertial load while retaining the other positive qualities of rubber-and-metal hinges. Figures 3, references 3 (Russian).

UDC 621.785.532:669.294

Mechanical Properties of Nitrided Tantalum at Increased Temperatures. T. A. Panayoti, candidate of technical sciences and docent, and S. G. Tsikh, graduate student, pp 109-113

This article investigates the effect of nitriding on the mechanical properties of type TVCh tantalum in the temperature interval from 800 to 1,200°C. Mathematical modeling is used to analyze the effect of temperature and the duration of machining on the mechanical properties of tantalum.

The effectiveness of using the method of saturating the surface with nitrogen to harden the tantalum is established. The ultimate strength of nitrided tantalum at the specified test temperatures is thus nearly doubled. Figures 2, tables 4, references 3 (Russian).

UDC 621.97

Investigation of Properties of Material With Heterogeneous Structure and Crossed Reinforcement. V. G. Kondratenko, candidate of technical sciences and docent, V. P. Gavryushenko, graduate student, and V. A. Artyukh, pp 113-117

This article presents the results of tests of a material of the system aluminum-boron with a geometric structure that has a crossed reinforcement. These data may be used to calculate the technological parameters of plastic metal working processes. Figures 2, table 1, references 3 (Russian).

UDC 621.73.011:539.374

Deformation Quality Criterion and Design of Rational Production Modes for Radial Forging. I. A. Dobychin, candidate of technical sciences and docent, and M. V.Ryvkin, graduate student, pp 117-120

This article proposes a deformation criterion for the quality of the metal of semifinished and finished products produced by plastic metal working. The criterion is represented as the indicator the the heterogeneity of the accumulated plastic deformation in the volume of the deformed body (or in some cross section). The dependence of the proposed criterion on technological and design parameters is analyzed on the basis of the authors' mathematical model of the process of drawing blanks on a radial forging machine (radial forging). Recommendations are made regarding selecting rational technological modes of the process of the radial forging of large titanium blanks. Figures 3, references 4 (Russian).

UDC 621.777.24.001

Determining Extrusion Force for Hollow Cylindrical Products Stamped in Accordance With Two-Channel Indirect Circuit. A. P. Bulanyy, candidate of physical and mathematical sciences and docent, and D. A. Dmitrenko, graduate student, pp 120-123

This article presents a refined mathematical model of the process of two-channel indirect extrusion of hollow cylindrical products. Figures 2, references 2.

UDC 621.73.043.001.63

Calculating Shape Change of Stiffening Ribs in Corner Zones. I. V. Kostarev, doctor of technical sciences and docent, and K. N. Solomonov, candidate of technical sciences, pp 123-125

This article develops a method of calculating the increase in stiffening ribs in corner zones in different stages of the formation of the shape of stamped forgings. The method is based on the theory of the flow of a thin plastic layer. The article proposes a specification of the form of the conditions contour in a form that makes it possible to eliminate jumps when calculating the height of stiffening ribs upon a transition from rectilinear sections of the actual contour to rounded sections in the specified zones and to thereby approximate the mathematical model of the process of shape formation to processes of the shape formation of ribbed components that are observed when they are produced by stamping under production conditions. Figure 1, references 3 (Russian).

UDC 621.983.011

Limit Deformations During Flaring of Anisotropic Pipes and Hole Deburring in Sheet Blanks. S. A. Shulga, candidate of technical sciences, and A. Yu. Averkiyev, candidate of technical sciences, pp 126-129

The stresses and strains in the vicinity of the edge are determined for processes of the flaring of thin-walled anisotropic tubes and the deburring of holes in sheet blanks. Also determined are the limiting degrees of shape change as a function of the parameters of force intensification, the characteristics of the mechanical properties, and the friction conditions on the contact surface.

The results of calculations based on the proposed dependencies conform to existing theoretical and experimental data. Figures 3, references 6 (Russian).

UDC 621.777.001.24

Shape Change and Forces of Bilateral Combined Extrusion. F. I. Antonyuk, pp 129-131

The upper estimate method is used to determine the specific forces of bilateral combined extrusion of hollow blanks with different wall thicknesses. Formulas are presented that make it possible to find the position of the metal flow's interface surface as a function of the geometric parameters of the blank and boundary conditions of the deformation. Figures 3, references 3 (Russian).

UDC 621.791.4:621.053:539.3

Achieving Optimum Pressure When Making Glued and Diffusion Joints. V. I. Kuzmenko, candidate of physical and mathematical sciences, pp 132-134

This article proposes an algorithm for calculating the distributed load at which the stresses arising on the surface of a glued or diffusion joint would be close to optimum. An example of solving the problem of the joint of a band and half-plane is presented. Figures 3, references 5 (Russian).

UDC 621.914.06-529:519.688

Asymptotically Optimum Algorithm for Approximating Curvilinear Contours by Orthogonal Nodes in Solutions of Milling Trajectory Problems. A.A. Ligun, doctor of physical and mathematical sciences/professor; A.A. Shumeyko, candidate of physical and mathematical sciences docent; V.S. Korotkov, graduate student, pp 135-138

This article develops an asymptotically optimum algorithm for approximating curvilinear contours by orthogonal nodes, which makes it possible, in the stage of programming milling, to control the precision of the trajectories of tools' motions in computer calculations. Figures 2, references 4 (Russian).

UDC 621.914.2.004.14

Kinematic Analysis of Process of Cutdown Milling. S. V. Chikin, engineer, A. L. Lepetyuk, candidate of technical sciences and docent, and I. G. Fedorenko, pp 139-142

This article examines a circuit for cutdown milling with different component and mill rotation speed ratios. The differences between the method of determining the maximum thickness of the cut layer of metal during cutdown milling and that used in the case of out-cut milling are specified, and graphs of the results of calculations based on the method are presented. It is established that, during machining at one and the same cutting speed, the loads on the mill are smaller in the case of cutdown milling than in the case of out-cut milling. Consequently, cutdown milling is more efficient than out-cut milling is. Figures 3, references 2 (Russian).

UDC 531.717.2

Measuring Geometric Parameters of Components by Difference Method. Yu. L. Nikolayev, candidate of technical sciences and docent, and A. G. Yershov, senior instructor, pp 143-147

This article examines the features of designing and constructing difference measuring schemes that make it possible to take simultaneous measurements of several geometric parameters while ensuring the relative elimination of affecting factors. Algorithms are presented for determining the measured functions in real time in a form that is convenient for programming. The article analyzes the methodological and specific components of instrument error and gives examples of using the method examined. Figures 3, references 2 (Russian).

UDC 621.9-529

Forming Specified Relative Arrangement of Surfaces During Turning on NC Lathe. O. F. Poltavets, candidate of technical sciences and docent, S. A. Zverkov, engineer, and S. I. Kucherenko, engineer, pp 147-152

This article proposes a method of forming rotation surfaces with a specified three-dimensional arrangement of their geometric axes during machining on an NC lathe.

Equations of the geometric axes of the formed surfaces with an allowance for the errors of the shape-forming motions of the tool and blank are derived on the basis of theoretical analysis. A dependency in discrete form is

derived for implementation of the process of controlling the formation of a specified arrangement of rotation surfaces based on the microprocessor system of an NC lathe. Figures 3, references 2 (Russian).

UDC 621.01

Method of Calculating Machining Precision With Allowance for Deformation of Production System's Components. N. P. Chernyanskaya, pp 152-157

This article proposes a method of calculating the deformation displacements of a production system's components and the related relative displacements of the tool and blank in the cutting zone, which makes it possible to determined the anticipated machining precision in the design stage. Figures 2, references 6 (Russian).

UDC 621.9.048.6

Optimizing Process of Vibratory Percussive Hardening. Yu. R. Konylov, candidate of technical sciences and docent, pp 157-160

This article examines the problems of optimizing the parameters of the process of vibratory percussive hardening of components with a complex shape when they are fastened to a container.

The analytical dependence of the main technological characteristics of the process (roughness, workhardness, residual compressive stresses, formation rate of plastic imprints) on the amplitude of the vibratory accelerations and frequency of the vibrations and compression of the vibrating working medium are shown. The optimization criterion and quasioptimal machining modes are determined. Figures 3, references 4 (Russian).

END OF FICHE DATE FILMED

31 May 1990